



Data report: X-ray fluorescence scanning of sediment cores, IODP Expedition 401 Site U1385, southwest Iberian margin (Portugal)¹

Contents

- 1 Abstract
- 1 Introduction
- 4 Methods
- 5 Results
- 8 Data availability
- 8 Acknowledgments
- 8 References

Keywords

International Ocean Discovery Program, IODP, *JOIDES Resolution*, Expedition 401, Mediterranean–Atlantic Gateway Exchange, Site U1385, Mediterranean Outflow Water, Messinian Salinity Crisis

References (RIS)

MS 401-202

Received 20 June 2025

Accepted 26 September 2025

Published 21 January 2026

Fadl Raad,² Patricia Standring,² Erwan Le Ber,³ Clara Blättler,² Isabelle Billy,⁴ Shamar Chin,² Manuel Teixeira,² Sarah J. Feakins,² Zhiyang Li,² Madeline Mulligan,⁵ Danielle Noto,² Jonathan Stine,² Xunhui Xu,² Jesse Yeon,⁶ Zakaria M. Yousfi,² Yunlang Zhang,⁷ Rachel Flecker,² Emmanuelle Ducassou,² Trevor Williams,² and the Expedition 401 Scientists²

¹Raad, F., Standring, P., Le Ber, E., Blättler, C., Billy, I., Chin, S., Teixeira, M., Feakins, S.J., Li, Z., Mulligan, M., Noto, D., Stine, J., Xu, X., Yeon, J., Yousfi, Z.M., Zhang, Y., Flecker, R., Ducassou, E., Williams, T., and the Expedition 401 Scientists, 2026. Data report: X-ray fluorescence scanning of sediment cores, IODP Expedition 401 Site U1385, southwest Iberian margin (Portugal). In Flecker, R., Ducassou, E., Williams, T., and the Expedition 401 Scientists, Mediterranean–Atlantic Gateway Exchange. *Proceedings of the International Ocean Discovery Program*, 401: College Station, TX (International Ocean Discovery Program). <https://doi.org/10.14379/iodp.proc.401.202.2026>

²Expedition 401 Scientists' affiliations. Correspondence author: fadl.raad@umontpellier.fr

³CNRS–Géosciences Montpellier–Campus Triolet, France.

⁴Environnements Paléoenvironnements Océaniques et Continentaux, UMR CNRS 5805, Université de Bordeaux, France.

⁵Department of Earth and Environmental Sciences, University of Iowa, USA.

⁶International Ocean Discovery Program, Texas A&M University, USA.

⁷Department of Earth Sciences, University of Southern California, USA.

Abstract

This report presents the results of X-ray fluorescence (XRF) scanning of sediment cores from International Ocean Discovery Program (IODP) Expedition 401 Site U1385, conducted as part of the Investigating Miocene Mediterranean–Atlantic Gateway Exchange (IMMAGE) Land-2-Sea drilling project. The expedition investigated Atlantic–Mediterranean exchange during the Late Miocene, focusing on the Messinian Salinity Crisis and its impact on climate and oceanography. Site U1385 is located on the Promontório dos Principes de Avis, a promontory extending west from the Portuguese margin in the northeast Atlantic, and recovered sediments from the lowermost Pliocene to the Tortonian. XRF scanning provides semiquantitative elemental data at a 2 cm resolution, revealing cyclic patterns in elemental abundances that reflect lithologies and can be correlated cyclostratigraphically with orbital cycles. These data highlight strong positive correlations among terrigenous elements (Al, Si, Ti, Mn, and Ba) and negative correlations between terrigenous and biogenic (Ca and Sr) elements. These results contribute to understanding the paleoceanographic and paleoenvironmental conditions at Site U1385 during the Upper Miocene and Lower Pliocene, providing insights into sediment provenance, diagenetic processes, and climatic variations.

1. Introduction

International Ocean Discovery Program (IODP) Expedition 401 is the offshore component of the Land-2-Sea drilling project Investigating Miocene Mediterranean–Atlantic Gateway Exchange (IMMAGE). During the expedition, conducted between December 2023 and February 2024, seven holes were drilled at four different sites: three sites in the Atlantic adjacent offshore Portugal (Holes U1609A, U1609B, U1610A, U1385K, and U1385L) and one site in the Alborán Sea just inside the Mediterranean (Holes U1611A and U1611B) (Flecker et al., 2025a). Here, we describe X-ray fluorescence (XRF) data from the two holes at Site U1385 (Figure F1).

Expedition 401 aimed to explore the history of Atlantic–Mediterranean exchange during the Late Miocene by targeting its geologic record from inception (~8 Ma) through the formation of the Mediterranean salt giant known as the Messinian Salinity Crisis (5.97–5.33 Ma; Ryan, 2009) and up to the establishment of an exchange configuration similar to present day (5–4 Ma). By analyzing offshore geologic records from these periods, the expedition’s key objectives included dating the time at which the Atlantic first started to receive a distinct outflow from the Mediterranean, assessing the impact of this outflow on Late Miocene climate, and testing physical oceanography models of extremely high density overflow dynamics. Site U1385 sediments were recovered back to approximately 8.8 Ma (Flecker et al., 2025a).

Site U1385 is located on a ridge, the Promontório dos Príncipes de Avis, and lies at a water depth of 2590 m, making it Expedition 401’s deepest site (Figure F1). It was first drilled in 2011 during Integrated Ocean Drilling Program Expedition 339 (Holes U1385A–U1385E) to provide a marine reference section for Pleistocene millennial climate variability. This initial drilling recovered a record that extends back to 1.45 Ma (at 151.5 meters below seafloor [mbsf]; Expedition 339 Scientists, 2013). Nearly a decade later, the same site was revisited during IODP Expedition 397 (in 2022) to extend the sequence back to the Miocene/Pliocene boundary (~5.3 Ma) at ~400 mbsf (Holes U1385F–U1385J), with the aim of reconstructing water mass changes during the Pliocene and Pleistocene (Hodell et al., 2024). The following year, Expedition 401 revisited Site U1385 again, drilling Holes U1385K and U1385L to extend coring through to the Late Miocene succession, with extended core barrel (XCB) drilling starting just above the Miocene/Pliocene boundary at ~400 mbsf. The aim was to document the nature, amplitude, and pacing of climate cycles in the Atlantic during the late Miocene and reconstruct water mass variability during this time period, which is characterized by extreme regional changes in oceanographic context.

Hole U1385K recovered Messinian and Tortonian deposits and reached a maximum depth of 552.5 mbsf. Hole U1385L reached 442.6 mbsf and recovered Early Pliocene and Late Miocene sediments (Flecker et al., 2025a). The recovered sediments at Site U1385 are characterized by alternating light greenish gray and greenish gray to gray beds of clayey calcareous ooze and calcareous clay (Flecker et al., 2025a).

XRF scanning of sediment cores from Site U1385 provides semiquantitative elemental concentrations that help to characterize the nature of the sediments, their provenance, and the underlying

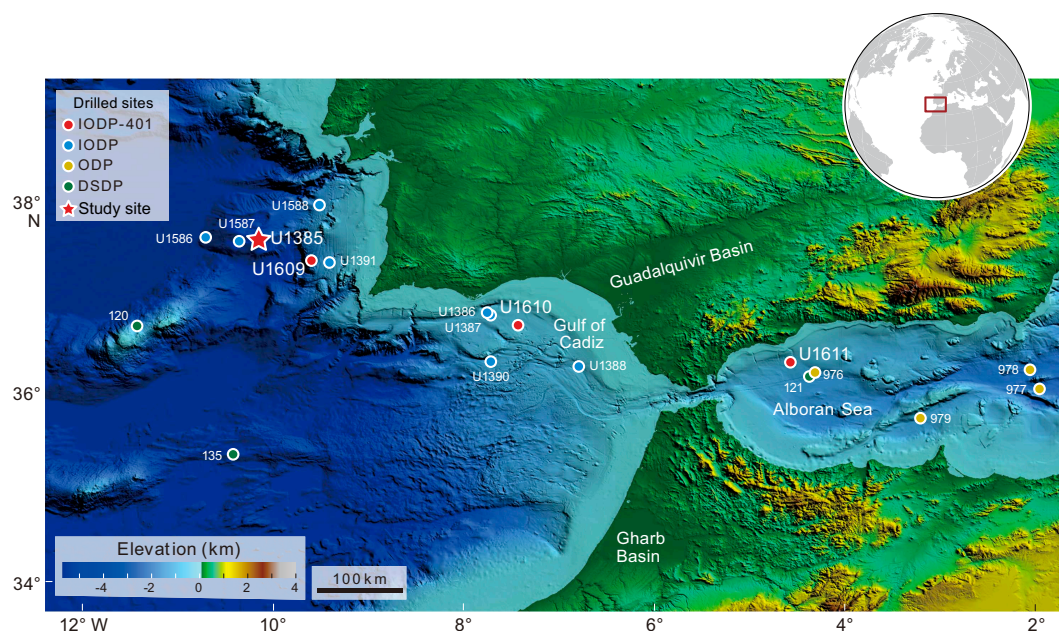


Figure F1. Topographic and bathymetric map of Gibraltar Strait region, showing locations of Site U1385 on southwest Iberian margin, other Expedition 401 sites, and sites from previous expeditions in Atlantic and Alborán Sea. ODP = Ocean Drilling Program, DSDP = Deep Sea Drilling Project. From Flecker et al. (2025a).

depositional processes. A scanning resolution of 2 cm was chosen for the purpose of reconstructing paleoceanographic and paleoenvironmental conditions (Rothwell and Croudace, 2015), as well as helping to interpret sediment provenance, diagenetic processes, and climatic variations during the Late Miocene.

This data report contains quality controlled XRF data combined with stratigraphic information to provide an overview of elemental abundance variability at Site U1385. Companion publications for the other Expedition 401 sites are also available (Sites U1609 [Teixeira et al., 2026], U1610 [Xu et al., 2026], and U1611 [Standring et al., 2026]). The data sets for the different holes at Site U1385 are plotted separately and not as splices because splices are still in development, incorporating shipboard and XRF data. Shipboard natural gamma radiation (NGR) and magnetic susceptibility (MS) data are shown for comparison. The shipboard age model indicated in Figures F2 and F3 is likely to be improved with postexpedition analyses.

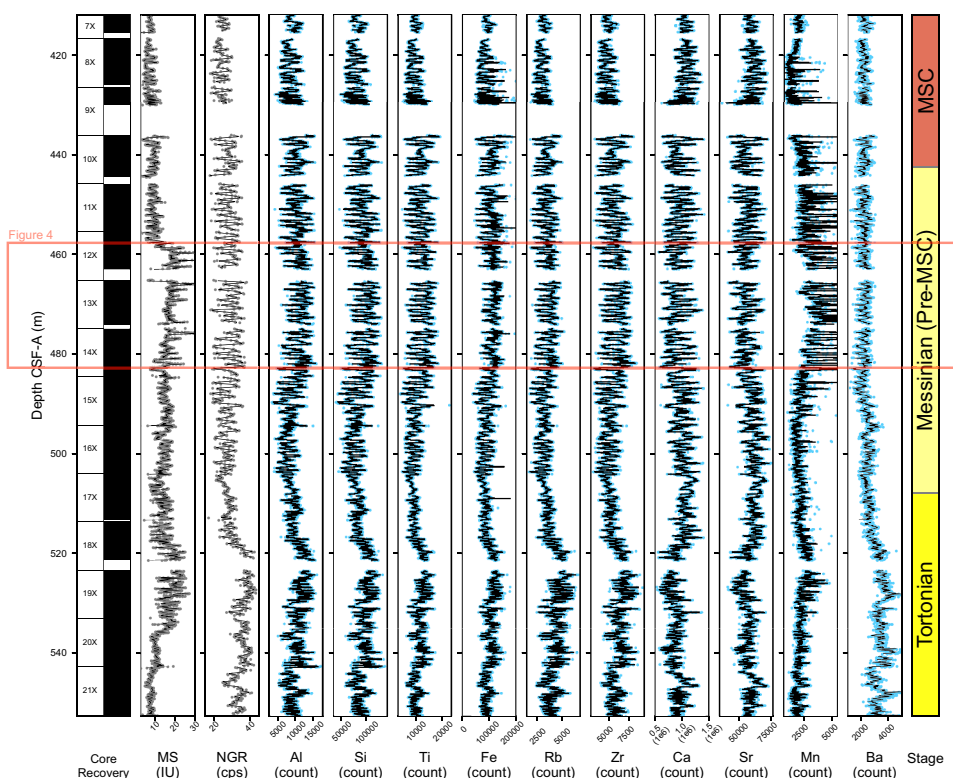


Figure F2. MS, NGR, and XRF counts of selected elements (Al, Si, Ti, Fe, Rb, Zr, Ca, Sr, Mn, and Ba), Hole U1385K. Age model used in this figure was generated on the ship (Flecker et al., 2025a). Gaps in data set correspond to incomplete drilling recovery. Dots = raw measurements. Solid lines = moving average with window set to 3 measurements. IU = instrument units, cps = counts per second, MSC= Messinian Salinity Crisis.

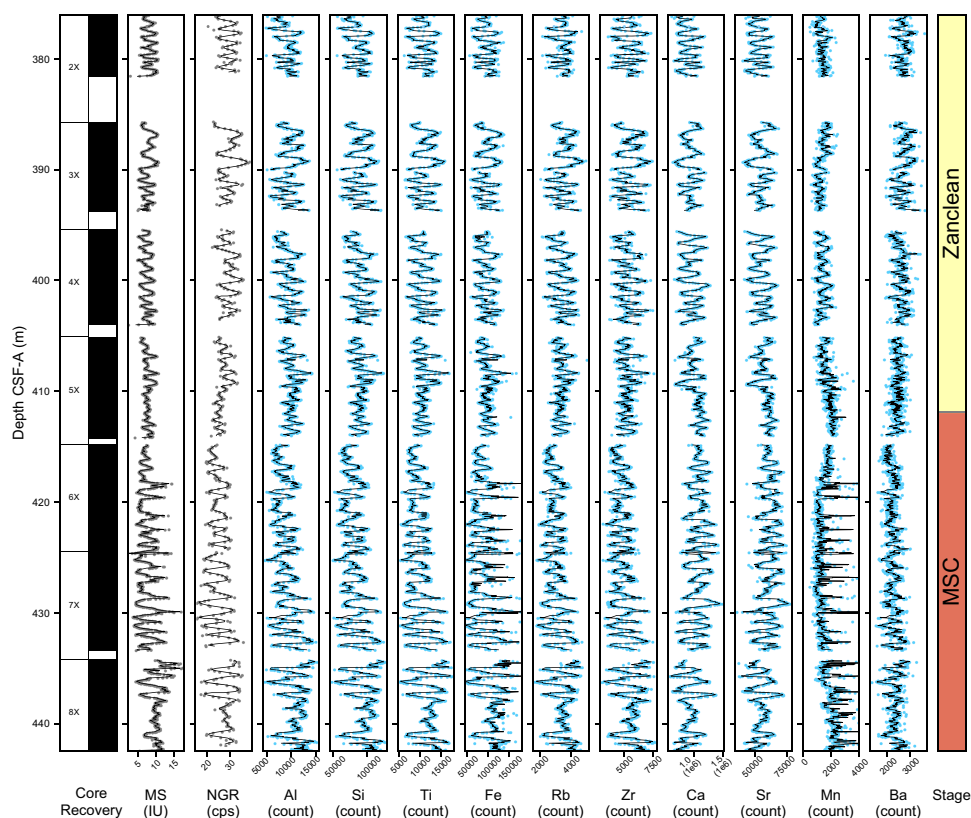


Figure F3. MS, NGR, and XRF counts of selected elements (Al, Si, Ti, Fe, Rb, Zr, Ca, Sr, Mn, and Ba), Hole U1385L. Age model used in this figure was generated on the ship (Flecker et al., 2025a). Gaps in data set correspond to incomplete drilling recovery. Dots = raw measurements. Solid lines = moving average with window set to 3 measurements. IU = instrument units, cps = counts per second, MSC= Messinian Salinity Crisis.

2. Methods

All the cores recovered from Holes U1385K and U1385L were scanned at the Gulf Coast Repository at Texas A&M University (USA) at a 2 cm resolution on the fourth-generation Avaatech Core Scanner (XRF2). The nondestructive method of XRF core scanning uses energy dispersive spectrometry to simultaneously measure photon energies through fluorescence of major, minor, and trace elements after excitation voltages of 10, 30, and 50 kV are directed at the core surface. The XRF2 scanner uses a water-cooled 100 W rhodium side Be-window X-ray tube, a Brightspec SiriusSD silicon drift detector, and a Topaz-X high-resolution digital multichannel analyzer. The measurement window slit size was set at 1 cm downcore by 1.2 cm cross-core. The enclosed prism that houses the detector was continuously flushed with helium to remove natural atmospheric contamination to reduce background noise in the data output. Archive halves of the sediment cores were scanned at 10 kV with no filter for major and minor elements (Al, Si, P, Cl, K, Ca, Ti, Mn, Fe, and Cr); at 30 kV with a thick Pd filter for additional major and minor elements, including geologically significant trace elements (K, Ca, Ti, Mn, Fe, Co, Ni, Zn, Br, Rb, Sr, and Zr); and at 50 kV with a Cu filter for heavier trace elements (Sr, Rb, Zr, and Ba).

In this report, the plotted elements Al, Si, Ca, Ti, Mn, and Fe are from the 10 kV scan; Rb, Sr, and Zr are from the 30 kV scan; and Ba is from the 50 kV scan.

2.1. Sediment core preparation

Prior to scanning, sediment cores were brought to room temperature to avoid later condensation that could cause X-ray attenuation (Tjallingii et al., 2007). Sediment cores were gently scraped with a glass slide across the width of the core to prevent contamination caused by smearing associated

with the protective film during storage, even the sediment surface ensuring good contact with the scanner, and remove any mold grown during storage. The glass slide was wiped clean between scrapes with a Kimwipe. The core was covered with a 4 μm thick Ultralene XRF film to prevent contamination as the XRF detector moves down the core and was smoothed using a roller nap to remove air bubbles. Each section was then leveled with the help of a spirit level after loading the core in the XRF core scanner to ensure measurement of a flat smooth surface. Any deviation from 0° can introduce air contamination.

2.2. Quality control

To ensure consistent data quality, a daily quality control was performed during XRF data acquisition by running standards at the three excitation levels used for elemental measurements (10, 30, and 50 kV). After warming up the scanner and before beginning measurements, 20 replicates were run at each excitation level. After completing the day's scanning, a single standard run was performed at each voltage and compared to the initial replicates to evaluate instrument performance and check for any film contamination. These standards were also utilized to evaluate instrumental bias in acquired count outputs and the operational reliability of the XRF core scanners.

Raw spectral peaks were processed and exported as counts per second for different elements using Brightspec's bAxilBatch software, uploaded into the IODP Laboratory Information Management System (LIMS) database, and then quality controlled by removing data points that exhibited high Ar values during the 10 kV measurement, indicating that air was measured rather than the core surface. The threshold count for the K- α of argon was set at 0, where any positive value was deemed unreliable and required further inspection or deletion, following standard laboratory practice. Typical values of argon averaged around $\sim 3,000$ counts, which signifies little to no atmospheric contamination. Some elements (e.g., Mg and Mo) were measured with the scanner but are not included in this data set due to low (i.e., <100 counts) detection, which was determined by negative or low count values. Although elemental values within two standard deviations of zero are typically removed from XRF data sets (Amadori et al., 2024), this criterion was not applied here. Given that signal strength can vary significantly between elements within the same sample (e.g., Ti counts may be meaningful but Ni counts may not be meaningful), the decision to exclude such values has been left to the discretion of the data user.

3. Results

Many features of the XRF data resemble the patterns visible in the shipboard physical properties data (Figures F2, F3). Both show pervasive cyclicity throughout Holes U1385K and U1385L, except for Mn, which commonly appears noncyclic. Regularly spaced medium- to high-amplitude (in term of counts) cycles characterize the youngest part of the recovered interval, such as the lowermost Pliocene and uppermost Messinian of Hole U1385L (Figure F3), with more variable frequency (i.e., cycle thicknesses) and lower amplitude cycles in intervals such as the lower Messinian and Tortonian stages of Hole U1385K (Figure F2).

The observed cyclicity is likely to be precessional and reflects the lithologic changes (clay–ooze alternation) in the Site U1385 cores (Flecker et al., 2025a). Typically, peaks in MS and NGR are in phase, and they coincide with peaks in terrigenous elements (Al, Si, Ti, Fe, and Zr) and troughs in biogenic elements (Ca and Sr) (Figure F4). An exception to this is the interval in Hole U1385K between ~ 458 and 482 m core depth below seafloor, Method A (CSF-A), where MS and NGR are out of phase (Flecker et al., 2025a). The correlation with the XRF elements in this interval remains the same, with troughs in NGR coinciding with troughs in terrigenous elements and peaks in biogenic elements. Interestingly, this interval coincides with a prominent increase in the Mn counts (Figure F2) and where Mn peaks reach relatively high counts ($>10,000$ counts; Figure F4). The interval with high manganese peaks also appears to be cyclic. The high manganese peaks are in phase with peaks in the biogenic elements Ca and Sr (Figure F3).

A series of scatter plots were used to assess the statistical correlations between different XRF elements at Site U1385 (Figure F5). These plots include all data points from Holes U1385K and U1385L. A Spearman's rank correlation was applied to determine the strength of the relationships

between individual element pairs (Figure F5). The nonparametric Spearman method is used to account for potential nonlinear relationships and nonnormal data distributions.

Elements typically linked to terrigenous sources have strong positive correlations such as between Al and Ti and between Si and Ti (Figure F5) and follow similar downhole trends (Figures F2, F3). The terrigenous elements (Al, Si, and Ti) have very strong correlations (e.g., $\rho = 0.99$ for Al and Si). Mn has a weak positive correlation with the terrigenous elements ($\rho = 0.21$ – 0.27). In contrast, biogenically sourced elements are negatively correlated with terrigenous inputs, as seen, for example, in comparisons between Al and Ca ($\rho = -0.62$) and between Si and Ca ($\rho = -0.69$). Barium is often used as a productivity proxy in marine sediments (Paytan et al., 1996) and has a positive correlation with terrigenous elements ($\rho = 0.42$ – 0.52) and a negative correlation with Mn and biogenic elements ($\rho = -0.042$ to 0.39). Ca and Sr have negative correlations when compared with terrigenous elements ($\rho = -0.53$ to -0.83).

The absence of correlation between Mn and the biogenic elements (Ca and Sr) appears to be largely influenced by the interval with elevated Mn counts shown in Figure F4. To test this, we crossplotted the XRF elemental data specifically within this interval (450–490 m CSF-A) and compared it with the crossplot in Figure F5. The result, presented in Figure F6, reveals a distinct difference: although Mn correlates positively with the biogenic elements in the high-Mn interval, this relationship is absent along the entire depth of Site U1385.

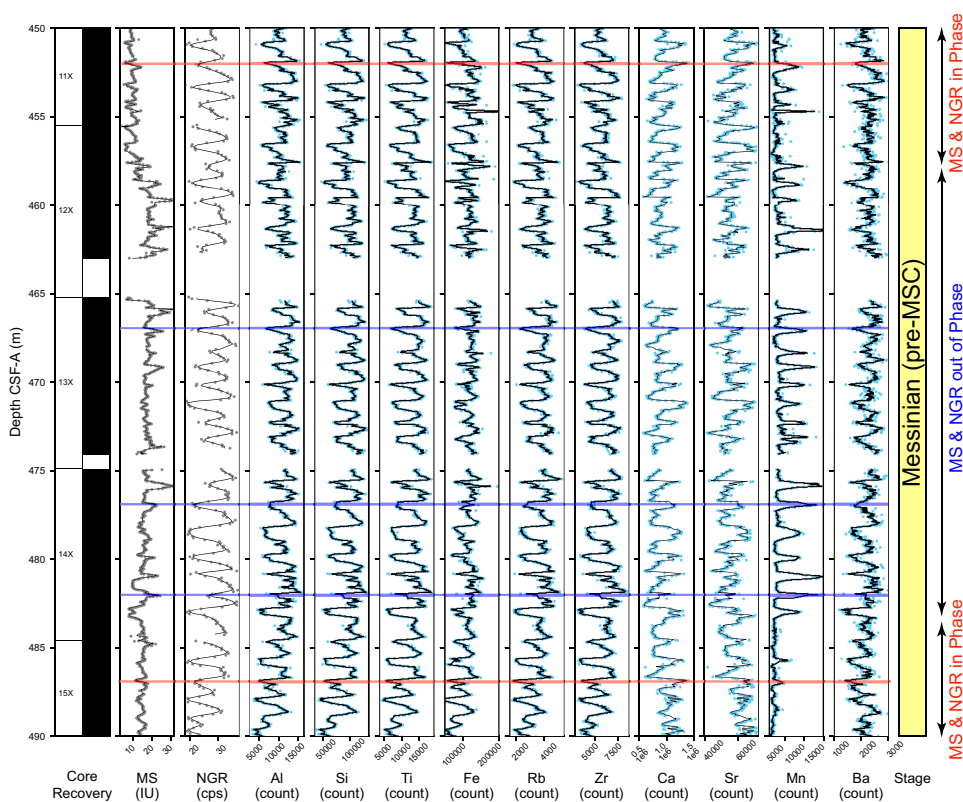


Figure F4. Close-up of MS, NGR, and XRF counts of selected elements (Al, Si, Ti, Fe, Rb, Zr, Ca, Sr, Mn, and Ba), Cores 401-U1385K-11X through 15X (see red square in Figure F2 for position). Red and blue lines are traced to show correlations between peaks and troughs for the measurements. Age model used in this figure was generated on the ship (Flecker et al., 2025a). Gaps in data set correspond to incomplete drilling recovery. Dots = raw measurements. Solid lines = moving average with window set to 3 measurements. IU = instrument units, cps = counts per second, MSC= Messinian Salinity Crisis.

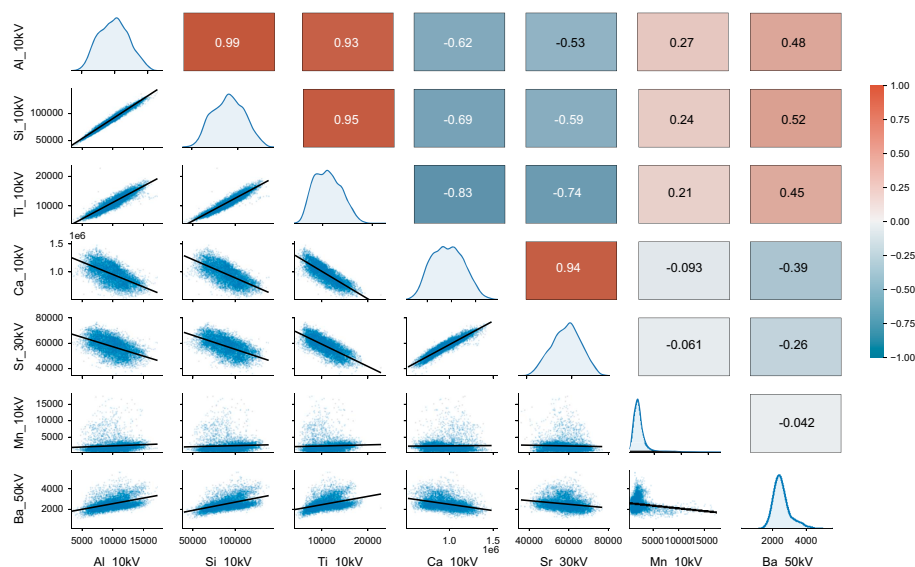


Figure F5. Lower left: crossplot matrix of selected XRF elements, Holes U1385K and U1385L. Matrix displays pairwise relationships between seven elements (Al, Si, Ti, Ca, Sr, Mn, and Ba). Diagonal panels show kernel density estimates for distribution of each element. Below the diagonal, scatter plots depict bivariate relationships, where each dot represents a measurement point and is semitransparent to reveal data density. Black lines = best-fit linear regressions for visualizing correlation trends. All data are filtered to exclude measurements influenced by residual argon signal contamination, yielding a total of 8833 quality controlled measurements. Upper left: Spearman rank correlation matrix of same elements. Heat map shows pairwise correlation coefficients between seven selected elements, with coefficients annotated in each cell. Correlations were computed using nonparametric Spearman method to account for potential nonlinear relationships and nonnormal data distributions. Color shading follows red–blue diverging color map centered at zero (red tones = positive correlations, blue tones = negative correlations). Strong positive associations are observed between several major elements, suggesting shared geochemical behavior or common sediment sources.

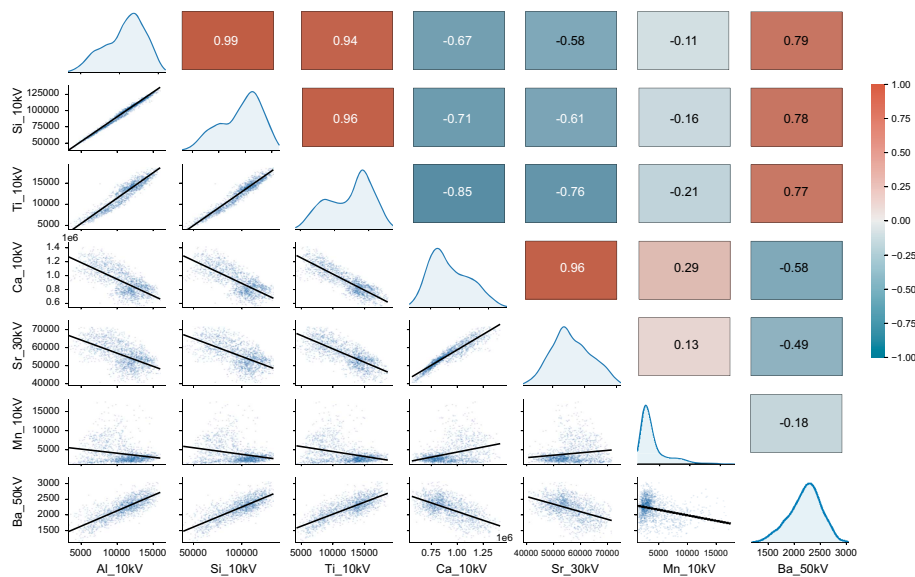


Figure F6. Lower left: close-up crossplot matrix of selected XRF elements at 450–490 m CSF-A shown in Figure F4, Hole U1385K. Matrix displays pairwise relationships between seven elements (Al, Si, Ti, Ca, Sr, Mn, and Ba). Diagonal panels show kernel density estimates for distribution of each element. Below the diagonal, scatter plots depict bivariate relationships, where each dot represents a measurement point and is semitransparent to reveal data density. Black lines = best-fit linear regressions for visualizing correlation trends. All data are filtered to exclude measurements influenced by residual argon signal contamination. Upper left: Spearman rank correlation matrix of same elements. Heat map shows pairwise correlation coefficients between seven selected elements, with coefficients annotated in each cell. Correlations were computed using the nonparametric Spearman method to account for potential nonlinear relationships and nonnormal data distributions. Color shading follows red–blue diverging color map centered at zero (red tones = positive correlations, blue tones = negative correlations). Strong positive associations are observed between several major elements, suggesting shared geochemical behavior or common sediment sources.

4. Data availability

Expedition 401 data are available at Zenodo (Flecker et al., 2025b).

5. Acknowledgments

This research utilized samples provided by the International Ocean Discovery Program (IODP). We extend our gratitude to the crew and technical staff of the R/V *JOIDES Resolution* during Expedition 401, as well as to the team at the Gulf Coast Repository, in particular Kara Vadman and Michelle Penkrot. The XRF scans presented here were part of the programmatic scanning for Expedition 401, funded by the National Science Foundation (NSF) through the U.S. Science Support Program (USSSP), which also provided travel support for United States scientists. Travel and accommodation support for F. Raad (correspondence author) was provided by IODP France. We are also grateful to Emily Estes for her constructive review and helpful comments on this report.

References

- Amadori, C., Borrelli, C., Christeson, G., Estes, E., Guertin, L., Hertzberg, J., Kaplan, M.R., Koorapati, R.K., Lam, A.R., Lowery, C.M., McIntyre, A., Reece, J., Robustelli Test, C., Routledge, C.M., Standring, P., Sylvan, J.B., Thompson, M., Villa, A., Wang, Y., Wee, S.Y., Williams, T., Yeon, J., Teagle, D.A.H., Coggon, R.M., and the Expedition 390/393 Scientists, 2024. Data report: X-ray fluorescence scanning of sediment cores, IODP Expedition 390/393 Site U1560, South Atlantic Transect. In Coggon, R.M., Teagle, D.A.H., Sylvan, J.B., Reece, J., Estes, E.R., Williams, T.J., Christeson, G.L., and the Expedition 390/393 Scientists, South Atlantic Transect. *Proceedings of the International Ocean Discovery Program, 390/393: College Station, TX (International Ocean Discovery Program)*. <https://doi.org/10.14379/iodp.proc.390393.205.2024>
- Expedition 339 Scientists, 2013. Expedition 339 summary. In Stow, D.A.V., Hernández-Molina, F.J., Alvarez Zarikian, C.A., and the Expedition 339 Scientists, *Proceedings of the Integrated Ocean Drilling Program, 339: Tokyo (Integrated Ocean Drilling Program Management International, Inc.)*. <https://doi.org/10.2204/iodp.proc.339.101.2013>
- Flecker, R., Ducassou, E., Williams, T., Amarathunga, U., Balestra, B., Berke, M.A., Blättler, C.L., Chin, S., Das, M., Egawa, K., Fabregas, N., Feakins, S.J., George, S.C., Hernández-Molina, F.J., Krijgsman, W., Li, Z., Liu, J., Noto, D., Raad, F., Rodríguez-Tovar, F.J., Sierro, F.J., Standring, P., Stine, J., Tanaka, E., Teixeira, M., Xu, X., Yin, S., and Yousfi, M.Z., 2025a. Expedition 401 summary. In Flecker, R., Ducassou, E., Williams, T., and the Expedition 401 Scientists, *Mediterranean–Atlantic Gateway Exchange. Proceedings of the International Ocean Discovery Program, 401: College Station, TX (International Ocean Discovery Program)*. <https://doi.org/10.14379/iodp.proc.401.101.2025>
- Flecker, R., Ducassou, E., Williams, T., Amarathunga, U., Balestra, B., Berke, M.A., Blättler, C.L., Chin, S., Das, M., Egawa, K., Fabregas, N., Feakins, S.J., George, S.C., Hernández-Molina, F.J., Krijgsman, W., Li, Z., Liu, J., Noto, D., Raad, F., Rodríguez-Tovar, F.J., Sierro, F.J., Standring, P., Stine, J., Tanaka, E., Teixeira, M., Xu, X., Yin, S., and Yousfi, M.Z., 2025b. IODP Expedition 401 X-ray fluorescence (XRF) [Data set]. *International Ocean Discovery Program*. <https://doi.org/10.5281/zenodo.16459854>
- Hodell, D.A., Abrantes, F., Alvarez Zarikian, C.A., Brooks, H.L., Clark, W.B., Dauchy-Tric, L.F.B., dos Santos Rocha, V., Flores, J.-A., Herbert, T.D., Hines, S.K.V., Huang, H.-H.M., Ikeda, H., Kaboth-Bahr, S., Kuroda, J., Link, J.M., McManus, J.F., Mitsunaga, B.A., Nana Yobo, L., Pallone, C.T., Pang, X., Peral, M.Y., Salgueiro, E., Sanchez, S., Verma, K., Wu, J., Xuan, C., and Yu, J., 2024. Expedition 397 summary. In Hodell, D.A., Abrantes, F., Alvarez Zarikian, C.A., and the Expedition 397 Scientists, *Iberian Margin Paleoclimate. Proceedings of the International Ocean Discovery Program, 397: College Station, TX (International Ocean Discovery Program)*. <https://doi.org/10.14379/iodp.proc.397.101.2024>
- Paytan, A., Kastner, M., and Chavez, F.P., 1996. Glacial to interglacial fluctuations in productivity in the equatorial Pacific as indicated by marine barite. *Science*, 274(5291):1355–1357. <https://doi.org/10.1126/science.274.5291.1355>
- Rothwell, R.G., and Croudace, I.W., 2015. Twenty years of XRF core scanning marine sediments: what do geochemical proxies tell us? In Croudace, I.W., and Rothwell, R.G. (Eds.), *Micro-XRF Studies of Sediment Cores: Applications of a non-destructive tool for the environmental sciences*. Dordrecht (Springer Netherlands), 25–102. https://doi.org/10.1007/978-94-017-9849-5_2
- Ryan, W.B.F., 2009. Decoding the Mediterranean salinity crisis. *Sedimentology*, 56(1):95–136. <https://doi.org/10.1111/j.1365-3091.2008.01031.x>
- Standring, P., Chin, S., Raad, F., Zhang, Y., Billy, I., Feakins, S.J., Li, Z., Mulligan, M., Noto, D., Stine, J., Teixeira, M., Xu, X., Yeon, J., Yousfi, M.Z., Flecker, R., Ducassou, E., Williams, T., and the Expedition 401 Scientists, 2026. Data report: X-ray fluorescence scanning of sediment cores, IODP Expedition 401 Site U1611, Alborán Sea. In Flecker, R., Ducassou, E., Williams, T., and the Expedition 401 Scientists, *Mediterranean–Atlantic Gateway Exchange. Proceedings of the International Ocean Discovery Program, 401: College Station, TX (International Ocean Discovery Program)*. <https://doi.org/10.14379/iodp.proc.401.204.2026>

- Teixeira, M., Chin, S., Standring, P., Zhang, Y., Billy, I., Feakins, S.J., Li, Z., Mulligan, M., Noto, D., Raad, F., Stine, J., Xu, X., Yeon, J., Yousfi, M.Z., Flecker, R., Ducassou, E., Williams, T., and the Expedition 401 Scientists, 2026. Data report: X-ray fluorescence scanning of sediment cores, IODP Expedition 401 Site U1609, SW Iberia Atlantic margin (Portugal). In Flecker, R., Ducassou, E., Williams, T., and the Expedition 401 Scientists, Mediterranean–Atlantic Gateway Exchange. Proceedings of the International Ocean Discovery Program, 401: College Station, TX (International Ocean Discovery Program). <https://doi.org/10.14379/iodp.proc.401.201.2026>
- Tjallingii, R., Röhl, U., Kölling, M., and Bickert, T., 2007. Influence of the water content on X-ray fluorescence core-scanning measurements in soft marine sediments. *Geochemistry, Geophysics, Geosystems*, 8(2):Q02004. <https://doi.org/10.1029/2006GC001393>
- Xu, X., Stine, J., Standring, P., Hernández-Molina, F. J., Billy, I., Chin, S., Feakins, S.J., Li, Z., Mulligan, M., Noto, D., Raad, F., Teixeira, M., Yeon, J., Yousfi, M.Z., Zhang, Y., Flecker, R., Ducassou, E., Williams, T., and the Expedition 401 Scientists, 2026. Data report: X-ray fluorescence scanning of sediment cores, IODP Expedition 401 Site U1610, Gulf of Cádiz, Atlantic. In Flecker, R., Ducassou, E., Williams, T., and the Expedition 401 Scientists, Mediterranean–Atlantic Gateway Exchange. Proceedings of the International Ocean Discovery Program, 401: College Station, TX (International Ocean Discovery Program). <https://doi.org/10.14379/iodp.proc.401.203.2026>